北京大学中国经济研究中心
China Center for Economic Research
讨论稿系列
Working Paper Series

E2022005 2022-05-07

Long-Term Impacts of COVID-19 on Air Quality : Insights from Human Travel Behavior

Susan Lu Yang Yao Shundong Zhang Jiaqi Zhao

Abstract：
Existing literature has shown that the outbreak of COVID-19 led to a significant improvement of air quality. However, whether such improvement will persist after reopening remains ambiguous. In this paper, we explore daily air quality and road congestion data in Chinese cities in 2020 and find that compared to the pre-pandemic level, daytime nitrogen dioxide concentration declined by 34.2 percent during the lockdown period, but it increased by 6.5 percent four months after reopening. This finding is consistent with the pattern of change in road congestion—traffic congestion decreased by 20.2 percent during the lockdown period and increased by 5.3 percent afterward. We find strong evidence of a significant shift in the mode of human travel from public transit to private vehicles. This suggests that the pandemic has encouraged travelers to avoid public transit and, thus, has exacerbated road congestion and air pollution in the long run.

Keywords: COVID-19, Air Pollution, Public Transportation, Travel Behavior
JEL Codes: I18, Q53, L91, R41

Long-Term Impacts of COVID-19 on Air Quality: Insights from Human Travel Behavior

Susan Lu* Yang Yao† Shundong Zhang ‡ Jiaqi Zhao§

March 27, 2022

Abstract

Existing literature has shown that the outbreak of COVID-19 led to a significant improvement of air quality. However, whether such improvement will persist after reopening remains ambiguous. In this paper, we explore daily air quality and road congestion data in Chinese cities in 2020 and find that compared to the pre-pandemic level, daytime nitrogen dioxide concentration declined by 34.2 percent during the lockdown period, but it increased by 6.5 percent four months after reopening. This finding is consistent with the pattern of change in road congestion—traffic congestion decreased by 20.2 percent during the lockdown period and increased by 5.3 percent afterward. We find strong evidence of a significant shift in the mode of human travel from public transit to private vehicles. This suggests that the pandemic has encouraged travelers to avoid public transit and, thus, has exacerbated road congestion and air pollution in the long run.

Keywords: COVID-19, Air Pollution, Public Transportation, Travel Behavior

JEL Codes: I18, Q53, L91, R41

*lu428@purdue.edu, Krannert School of Management, Purdue University.

†yyao@nsd.pku.edu.cn. National School of Development, Peking University and China Center for Economic Research (CCER), Peking University.

‡zhangshundong@pku.edu.cn. National School of Development (NSD), Peking University and China Center for Economic Research, Peking University.

§jqzhao2017@nsd.pku.edu.cn. National School of Development, Peking University and China Center for Economic Research (CCER), Peking University.

1 Introduction

Recent studies show that COVID-19 had positive impacts on air quality in the short term. Road congestion and air quality improved when production and travel were suspended because of the lockdown (Dang and Trinh, 2020; Fan et al., 2020; He et al., 2020; Ming et al., 2020). The pandemic also encourages the popularity of remote work (Bartik et al., 2020; Dingel and Neiman, 2020), and existing studies have shown that remote work alleviates traffic congestion and air pollution (Pérez et al., 2004; Giovanis, 2018).

However, the widespread impacts of COVID-19 could invite behavioral changes in travel patterns that may in turn worsen air quality. For example, during the pandemic, people become much more cautious about taking public transit, such as buses and subways, because of the fear of being infected. As a result, many people may shift to private vehicles when they travel in the city (Abdullah et al., 2020; Bucsky, 2020; Kwok et al., 2020). If such changes persist over time, road congestion will worsen. This issue is well documented by the literature—motor vehicle emissions contribute a significant portion of air pollution, especially in metropolitan areas (Chan and Yao, 2008; Yang et al., 2011). Traffic congestion particularly exacerbates air pollution because it leads to frequent stops and acceleration (Zhang and Batterman, 2013). Thus, reducing traffic congestion can have substantial impacts on air quality and public health (Currie and Walker, 2011). One way to reduce congestion is to promote public transportation. Studies show that public transportation, compared to private vehicles, can effectively reduce the volumes of volatile organic compounds and NOx (Shapiro et al., 2016). If the pandemic indeed led to a shift in how people travel from public transit to private vehicles, then air quality would worsen in the long run.

In this paper, we investigate the short- and long-term impacts of the COVID-19 pandemic on the main pollutant caused by vehicles, nitrogen oxide (NO_2), and traffic congestion in China and link them to changed human travel behavior. China is one of the few countries that has controlled the nationwide spread of the pandemic since March 2020, which allows us to use a difference-in-differences (DID) approach to study the dynamic impacts of the pandemic on air pollution and human travel behavior before and after the pandemic was contained.

First, we investigate the impact of the COVID-19 pandemic on road congestion and NO_2 concentration in different stages of the development of the pandemic. Consistent with previous studies, we find that congestion and daytime NO_2 concentration dropped by 20.2 percent and 34.2 percent, respectively, during the lockdown period. However, the improvements disappeared when local governments terminated their lockdown policies. Our results show that compared to the pre-pandemic levels, the city congestion index and daytime NO_2

concentration increased by 5.3 percent and 6.5 percent, respectively, sixteen weeks after the end of lockdown. Although the pandemic led to short-term improvements, mostly because of the significant reduction of socioeconomic activities, it worsened air quality in the long run. The results remain robust under different specifications, measures, and samples.

The long-term increase in road congestion suggests that the COVID-19 pandemic might have caused some persistent changes in human travel behavior. Indeed, we find evidence for the shift in the mode of human travel from public transit to private vehicles. The outbreak of the pandemic raises the relative cost of taking buses and subways because of the potential risk of infection, which encourages people to rely more on private vehicles for daily transportation. Once people adapt to that mode of travel, inertia may prevent people from shifting back. Consistent with this explanation, we obtain three pieces of supporting evidence. First, the number of public transit passengers in 36 major cities has not recovered to pre-pandemic levels even six months after reopening, and auction prices of license plates continues to grow. Second, using daily subway passenger data in eight metropolitan areas, we find that the volume of subway passengers 16 weeks after reopening was 22.7 percent lower than the pre-pandemic level, while road congestion rose by 10.3 percent during the same period. Third, a heterogeneous analysis using the nationwide sample shows that the rise of daytime NO_2 emission only appeared in cities with high densities of public transit before the pandemic.

Our study makes two contributions. First, we contribute to a growing literature that explores the effects of COVID-19 policies on air quality. Recent studies have shown that interventions to contain the spread of COVID-19, such as lockdown, social distancing, and stay-at-home policies, significantly reduced the concentration of pollutants and improved air quality in the short run (Dang and Trinh, 2020; Fan et al., 2020; He et al., 2020; Ming et al., 2020; Otmani et al., 2020; Singh and Chauhan, 2020; Venter et al., 2020; Almond et al., 2021; Brodeur et al., 2021; Ju et al., 2021; Ropkins and Tate, 2021). The literature also shows that the improvement was heterogeneous across regions (Kerr et al., 2021). However, those studies do not address the long-term effects of the pandemic on human behavior and their consequences on air quality. Finding that the pandemic changed human travel behavior, we make a significant contribution to this line of literature. Second, our study provides nuanced insights to the literature on public transportation systems. Public transportation is considered an effective solution to road congestion and air pollution (Chen and Whalley, 2012; Topalovic et al., 2012; Anderson, 2014; Bel and Holst, 2018; Gendron-Carrier et al., 2018; Li et al., 2019; Gu et al., 2021). Studies have found that the demand for public transportation sharply declined during the pandemic (Kim et al., 2017; Abdullah et al., 2020; Kwok et al., 2020; Liu et al., 2020). It is unclear, though, whether the decline is

temporary or long-lasting. Our findings suggest that the decline could be long-lasting and, thus, imposes a great challenge for policymakers to recover the public's confidence in the demand for public transit.

We have organized the rest of the paper as follows. Section 2 summarizes the timeline of the COVID-19 pandemic in China. Section 3 introduces the sample, data, and empirical strategy used in this paper. Section 4 presents the main findings on traffic congestion and air pollution. Section 5 studies the shift of travel patterns as one potential mechanism. Section 6 concludes the paper.

2 The Timeline of COVID-19 in China

Figure 1 displays the timeline of the pandemic in China. On January 20, 2020, Dr. Nanshan Zhong disclosed on national television that the new coronavirus pneumonia was transmissible between people. On January 23, the Wuhan government mandated a city-wide lockdown, starting the first public intervention in response to the COVID-19 outbreak in the world. Subsequently, many other cities in China started lockdown. The central government also adopted several effective measures to contain the spread of the virus, including increasing capacity in intensive care units, building temporary hospitals, and setting up safety bubbles for COVID-19 patients with mild conditions (Chen et al., 2020; Chinazzi et al., 2020; Pan et al., 2020; Tian et al., 2020).

The outbreak of the pandemic coincided with the 2020 Chinese Spring Festival. The Spring Festival holiday was supposed to last for one week, from January 24 to January 30, right after Wuhan's lockdown. Because of the pandemic, the government decided to extend the holiday breaks and mandate citizens to stay at home. Lockdown mostly took the form of community close-off. In Chinese cities, most residents live in walled residential communities, which made lockdown easier. The enforcement of lockdown varies across cities. The strictest lockdown requires people to stay in their individual communities, and the government sends daily supplies to the door of each community. The least strict lockdown

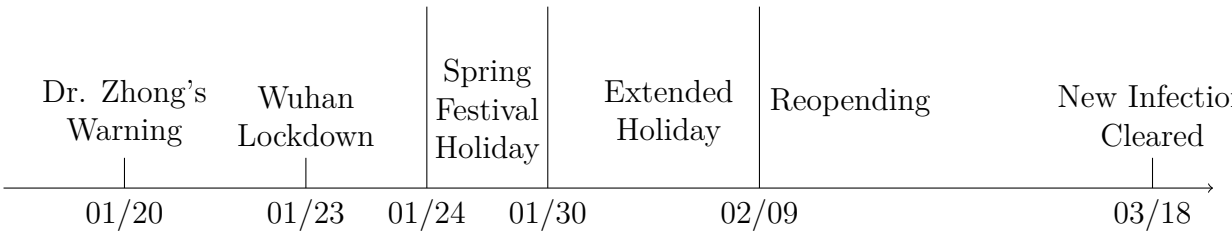

Figure 1: The Timeline of the COVID-19 Pandemic in China

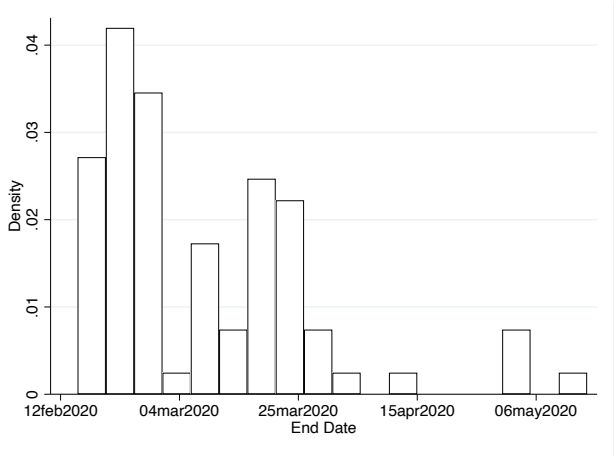

Figure 2: The Distribution of Lockdown End Dates

allows people to go out but restricts the entry of nonresidents. When the spread of the virus was seemingly contained, the central government recommended reopening of industrial production on February 9, 2020. Workers went back to work gradually. On February 19, the central government advised nationwide reopening. On March 18, the number of new infections dropped to zero, indicating the end of the nationwide pandemic. By May 13, all cities were reopened (Figure 2). [1]. China's restrictive quarantine policy effectively isolated the country from outbreaks in other countries. There were isolated outbreaks in some cities after March 2020, but the country as a whole has been set free from the pandemic. This provides a good setting for us to separate the pandemic's short-term and long-term effects.

3 Data and Methodology

3.1 Data

We use three main data sources. The air quality data, maintained by the China National Environmental Monitoring Centre (CNEMC), provides hourly pollutant measures at the city level. The traffic congestion data is maintained by Gaode Map, a leading web mapping service provider, and provides daily congestion information. We also collect temperature, humidity, atmospheric pressure, and wind speed information from the US National Climatic Data Center. All three datasets are constructed at the city-daily level. We use their location information to merge the three datasets. We also manually collected the lockdown information across cities and obtained public transportation information before the pandemic

[1]There was no more lockdown in our data period. There have been scattered lockdowns afterward but their scale and duration were much smaller than the first wave of lockdown.

Table 1: Summary Statistics

Variable	Obs	Mean	Std. dev.	Min	Max
NO_2, 24-hourAverage ($\mu g/m^3$)	44,388	32.58	17.43	3.00	128.00
NO_2, Daytime ($\mu g/m^3$)	44,388	27.75	16.38	2.09	138.45
NO_2, Night ($\mu g/m^3$)	44,388	36.42	19.78	2.54	136.77
Congestion Index	44,388	1.51	0.21	1.00	4.05
Air Temperature	44,388	14.48	10.17	-25.73	34.35
Dew Point Temperature	44,388	7.66	11.81	-35.56	28.85
Sea-level Pressure	44,388	1,017.50	9.76	987.56	1,055.83
Wind Direction	44,388	165.94	66.10	0.00	360.00
Wind Speed	44,388	2.63	1.33	0.00	18.00
Precipitation	44,388	2.47	8.51	0.00	209.10
Public Transit Density	43,292	74.70	90.54	3.41	478.02

and daily subway passenger volumes in eight metropolitans. Table 1 reports the summary statistics of the variables.

Emission and traffic congestion are seasonal. To control for seasonal fluctuations, we construct a two-year panel for our study. The main sample includes 44,388 observations and covers 81 locked-down cities in China between 100 days before and 173 days after the Spring Festival in 2019 and 2020. The lunar New Year was February 5th in 2019 and January 25th in 2020, so our dataset contains observations during October 28, 2018–July 28, 2019 (year 2019) and October 17, 2019–July 16, 2020 (year 2020). [1] In this construction, the days of year 2020 are considered the treatment group and the days of year 2019 are considered the control group. In our analysis, dates are defined relative to the lunar New Year.

Our main analysis rests on the 81 locked-down cities because they have both air pollution and congestion data, and we can create a balanced panel. Figure 3 displays the sample cities. Most of the cities are either located on the eastern coast or the economic centers in inland provinces. Therefore, the results of congestion should be considered as estimations for relatively developed and large cities, not the average effects of the entire country. In Section 4.3, we release this restriction by expanding the sample to all cities that have NO_2 observations.

Air Pollution.— We obtain air pollution data from CNEMC, which publishes city-level real-time air quality data (such as air quality index, NO_2, SO_2, O_3 and particulates) at daily and hourly levels. The variables are measured as concentration indexes of air pollutants ($\mu g/m^3$). In this paper, we mainly focus on NO_2, SO_2. All fossil fuels, such as coal, oil, gas, and diesel, generate NO_2, SO_2 when they are burned at high temperatures. Fire power

[1] July 16, 2020, is the last date of our data collection.

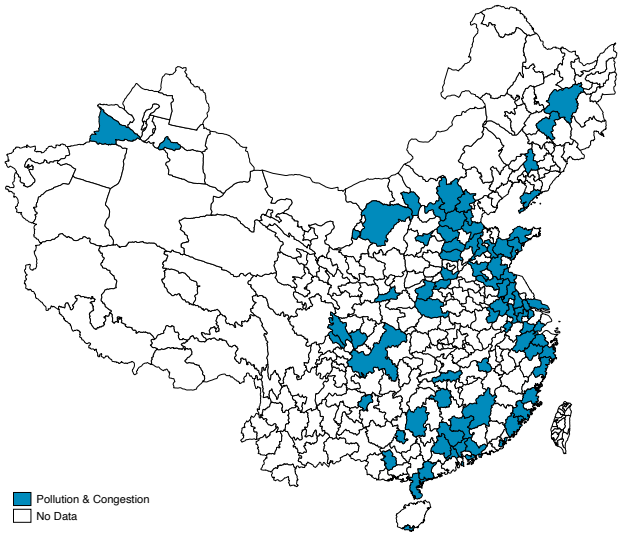

Figure 3: Cities in the Main Sample

stations and vehicular exhaust are the two major sources of NO_2, SO_2 in most Chinese cities. In 2019, vehicular exhaust contributed 51.4 percent of NO_2 emission in China. [1] When the use of fire power is controlled for, NO_2 concentration is mostly related to people's travel patterns. In Section 4.3, we study the changes in other pollutants. We drop cities with more than 100 missing values in NO_2 to minimize the problem of missing values. For the remaining cities, we fill in the missing values by using the value of the nearest day before.

Figure 4(a) hows the daily 24-hour average concentration of NO_2 in 2019 and 2020. The dashed line represents NO_2 concentration in 2019. As expected, emission declined in warmer months. The solid line represents NO_2 concentration in 2020. Before the outbreak, emission was quite similar to 2019 but plummeted immediately after the outbreak. It reached the bottom around February 9, 2020, when the national work resumption order was announced, and then quickly rebounded to the 2019 level. We found no systematic gaps for the two years. Figure 4(b) presents the comparison for the daytime period (8 AM–7 PM). Although daytime NO_2 followed a similar pattern to the 24-hour average, it reached a level slightly higher than the 2019 level 120 days after the Spring Festival.

City Congestion and Delay Index. – The key traffic congestion measure is the congestion and delay index (CDI), which is constructed by Gaode Map using the traffic information collected by the company's satellite data. According to the 2020 Gaode Chinese Major City Transport Report, [2] the CDI is defined as the ratio between the actual flow time in a certain

[1] See Ministry of Ecology and Environment of China, "Annual Report of Ecology and Environment Statistics of China (2019)" (in Chinese), accessed on August 11, 2020, https://www.mee.gov.cn/hjzl/sthjzk/sthjtjnb/202108/t20210827_861012.shtml.

[2] See Gaode Map, "2020 Gaode Chinese Major City Transport Report" (in Chinese), accessed on February

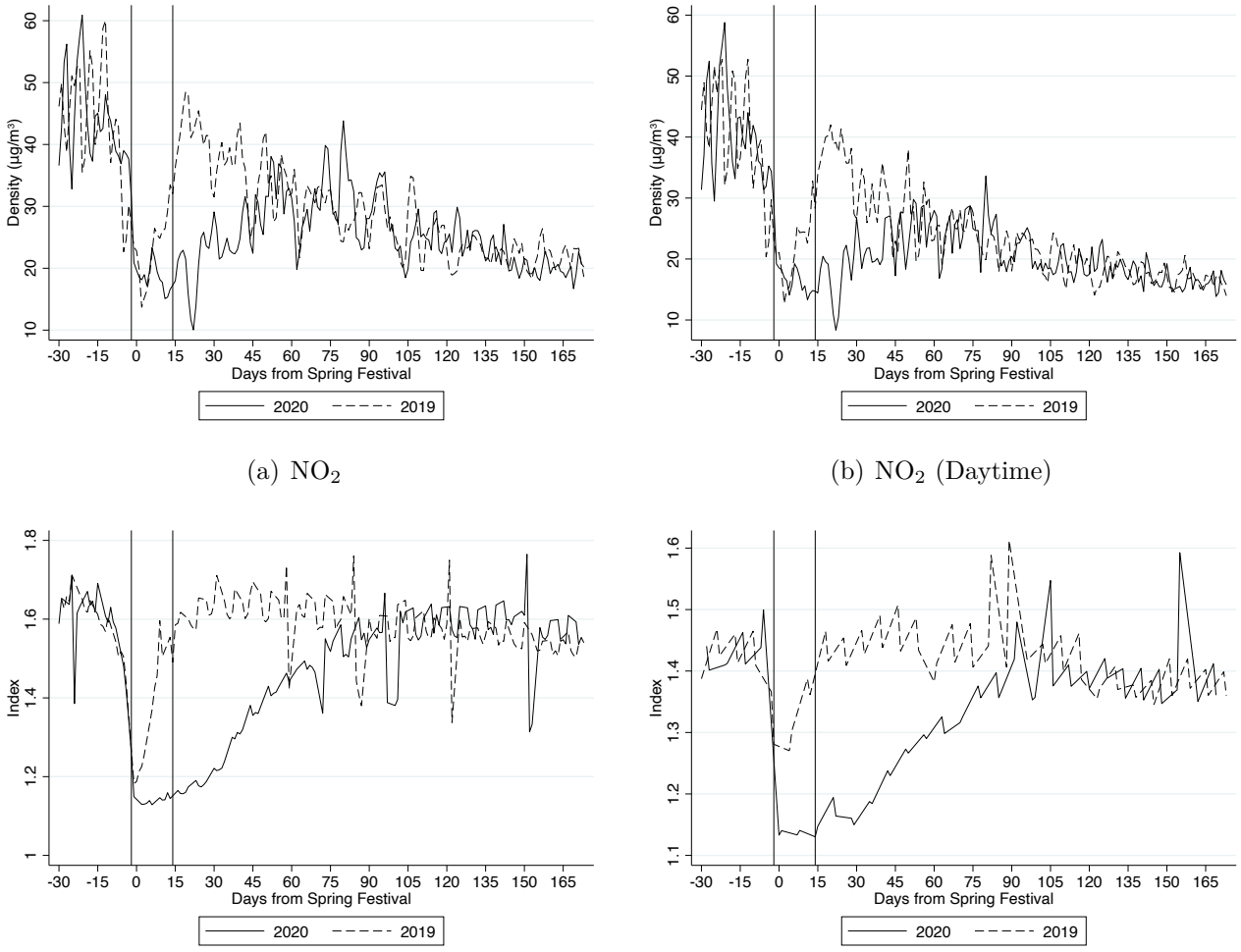

(a) NO_2

(b) NO_2 (Daytime)

(c) Congestion (Weekday)

(d) Congestion (Weekend)

Figure 4: The Time Trends of Dependent Variables

Note: The vertical lines represent the beginning and the end of the Spring Festival holiday in 2020.

length of time and the flow time without congestion for that length of time. The latter is a historical average. Gaode only publishes daily CDI. A higher value of CDI indicates heavier average traffic in a day. The measure covers 100 cities in China and is widely used as a congestion measure in the literature (Yan et al., 2020). We match the congestion index with pollution data, and finally, we include 81 cities in our sample.

Figure 4(c) and 4(d) display the trends of CDI on weekdays and weekends in 2019 and 2020. The dashed line is for 2019, and the solid line is for 2020. Like NO_2, the two years were quite identical before the outbreak of the pandemic. CDI plummeted immediately after the outbreak in 2020 and reached the bottom also on February 9, 2020. However, CDI bounced back more strongly than NO_2, and 120 days after the Spring Festival, it exceeded the 2019 level on the same day, indicating that enduring changes might have happened in people's travel patterns.

Lockdown Period.— China maintains a dynamic lockdown policy tailored to the local situation. Local governments are responsible for implementing their lockdown policies. As such, the lockdown period in our analysis varies from city to city. We assign the date of the Wuhan lockdown (January 23, 2020, or December 29, 2019, in the Chinese lunar calendar) as the beginning of the lockdown policy for all cities. Most cities implemented primary control policies, such as travel restrictions, closing public places, and community close-off, right after the announcement of Wuhan's lockdown. By late January, all provinces had activated the first-degree public health emergency responses. After activating first-degree responses, municipal governments are formally authorized by the provincial government to implement strict disease control policies, including large-scale lockdowns.[1]

We searched on government websites and local news reports to determine the end of lockdown in each city. As a general rule, we chose the date when a city government announced stopping community seal-off as the end of the city's lockdown. We do not distinguish the severity of community seal-off. If that date is unavailable, we use the date when the city government decided to start the "precise control policy," which usually means the lockdown policy would only exist in communities with confirmed cases. If that date is still not available, we then use the end of the province's first-level responses as the end date of a city's lockdown. As shown in Figure 2, most cities ended lockdown before April although some did not until May. In Section 4.3, we explore alternative definitions of the lockdown period.

Control Variables.— We consider a series of meteorological control variables that affect air quality and traffic congestion. For example, rains may change people's choices about transportation methods and affect air quality as well. To relieve this concern, we collect

13, 2022, https://report.amap.com/share.do?id=a187527876d07ac50177142eba987ce0.

[1]See http://www.gov.cn/yjgl/2006-02/26/content_211654.htm.

data from the US National Climatic Data Center for site-level daily weather conditions. We match each city to the closest site according to the distance from the city center to the site. If no site appears within 100 km from the city center, we exclude the city from our sample. For each city, we generate six daily weather variables: temperature, humidity, precipitation, sea-level pressure, wind speed, and wind direction. Similar to NO_2 concentration, we drop cities with more than 100 missing values in any weather variable. For the remaining cities, we fill in the missing values by using the value of the nearest day before.

3.2 The Empirical Strategy

Following He et al. (2020) and Almond et al. (2021),we apply the DID model to examine the impact of COVID-19 on air quality and human mobility. The unit of observation in our analysis is the city-day observation and the baseline model is specified as follows:

$$lnY_{cdt} = \gamma_0 + \sum_{i=0}^{3} \beta_i COVID_t \times Stage_{icd} + \sum_{i=0}^{3} \theta_i Stage_{icd} + \gamma_1 X_{cdt} + \delta_{ct} + \zeta_d + \epsilon_{cdt} \qquad (1)$$

The dependent variable, Y_{cdt}, refers to congestion measures or air quality in city c in the Chinese lunar calendar day d of year t. $COVID_t$ indicates the treatment group (year 2020). That is, it is a binary variable that equals 1 if day d was in 2020, the year of the pandemic, and 0 if day d was in 2019. In the regression, the sample window ranges from 100 days before the Spring Festival to 173 days after the festival in 2019 and 2020.

The pre-treatment period contains days before the lunar calendar day December 29 (Wuhan's lockdown date in 2020). Instead of studying the average treatment effect of COVID-19, we study its dynamic effects. Thus, we divide the treatment period into four stages according to the development of the pandemic. $Stage_{0cd}$ refers to the city-specific lockdown period in city c,— that is, the lunar calendar days from the lunar calendar day December 29 to the end of city c's lockdown. Different cities had different termination dates. The following days are divided by an 8-week interval. Days covered by $Stage_{1cd}$ include the initial period when workers came back to work and when industrial activities resumed right after the COVID-19 pandemic. Subsequent stages are conveniently arranged to follow the rhythm of this initial stage. The coefficients β_i's allow us to observe the dynamic impacts of COVID-19. Specifically, β_0 measures the immediate lockdown effect, β_1 measures the short-term aftermath effect during the initial opening stage, and β_2 and β_3 measure the long-term aftermath effects when economic and social activities came back to normal.

X_{cdt} includes a set of time-varying city-level characteristics, including weather conditions (daily temperature, humidity, sea-level pressure, wind speed, and wind direction) and holiday

fixed effects.[1]. We also control for the lunar day fixed effect (ζ_d). In addition, we control the city-year fixed effect (δ_{ct}), which allows us to conduct our comparison within the city. It is by far the most stringent comparison that we can reach. The standard errors are clustered by city.

To make sure that the coefficients β_i's estimated from Equation 1 are not caused by the trends existing before the pandemic, we estimate the following event-study specification:

$$lnY_{cdt} = \gamma_0 + \sum_{i=-4, i\neq -1}^{n} \beta_i COVID_t \times T_{icd} + \sum_{i=-4, i\neq -1}^{n} T_{icd} + \gamma_1 X_{cdt} + \delta_{ct} + \zeta_d + \epsilon_{cdt} \qquad (2)$$

Here, T_{icd} indicates periods. It is defined differently before and after the lunar calendar day December 29. It equals 1 if date d is within i month before lunar calendar day December 29, and 0 otherwise. The omitted period is the month before the lunar calendar day December 29. The constant γ_0, associated with this month, captures the base difference between 2019 and 2020. For days after December 29, T_{0cd} is defined as the same as $Stage_{0cd}$ in Equation 1. $T_{icd}(i \geq 1)$ refers to the ith week after the lockdown period. The set of coefficients β_i's $(i < 0)$ capture the pre-pandemic time trend of the differences between 2019 and 2020. If the coefficients are not different from zero, we then conclude that the effects of COVID-19 estimated from Equation 1 are not caused by pre-existing trends.

4 NO_2 Emission and Traffic Congestion

As pointed out in the introduction, the literature well documents the link between traffic congestion and pollution. We will not repeat this link. In this section, we study how NO_2 emission and traffic congestion perform over different periods of the pandemic, based on the specifications in Equations 1 and 2 . In the next subsection, we will explore the causes for the changes in traffic congestion by studying the pandemic's impacts on people's travel behavior.

4.1 NO_2 Emission

We estimate Equation 1 using both the full sample and the sample of weekdays only and report the results in Table 2. Columns (1)–(3) present the results of the full sample, and Columns (4)–(6) present the results of the weekday sample. For each sample, we examine three measures of NO_2 concentration in log transformation: 24-hour average, daytime

[1]The main holidays covered by our data are the Qingming Festival, Labor Day, and Dragon Boat Festival.

Table 2: The Results for NO_2

Outcome	Log NO_2					
	Full Sample			Weekdays Only		
	24 hour	Day	Night	24 hour	Day	Night
	(1)	(2)	(3)	(4)	(5)	(6)
Lockdown	-0.350***	-0.342***	-0.355***	-0.306***	-0.283***	-0.304***
	(0.000)	(0.000)	(0.000)	(0.000)	(0.000)	(0.000)
Weeks 1–8	-0.003	0.028	-0.024	-0.037	0.014	-0.057*
	(0.907)	(0.194)	(0.300)	(0.098)	(0.541)	(0.022)
Weeks 9–16	0.053**	0.060**	0.039*	0.019	0.059**	0.002
	(0.004)	(0.002)	(0.047)	(0.304)	(0.003)	(0.942)
Weeks >16	0.010	0.065*	-0.034	-0.008	0.045	-0.043
	(0.745)	(0.046)	(0.297)	(0.825)	(0.193)	(0.257)
Observations	44,388	44,388	44,388	31,671	31,671	31,671
R^2	0.679	0.669	0.641	0.687	0.676	0.649

Note: *p*-values are reported in parentheses. Standard errors are clustered at the city level. Control variables include daily temperature, humidity, sea-level pressure, wind speed, wind direction, city-year fixed effects, and lunar calendar date fixed effects. Day: 8:00-19:00. Night: 0:00–8:00 and 19:00–24:00. Lockdown: lockdown period. * $p < 0.05$, ** $p < 0.01$, *** $p < 0.001$.

average, and nighttime average, respectively.

The results in Column (1) suggest that lockdown helps reduce NO_2 by 35 percent in the full sample. This result is consistent with the existing literature on the short-term impacts of COVID-19 on pollutants in China (Fan et al., 2020; He et al., 2020; Ming et al., 2020; Almond et al., 2021). After reopening, however, the impact fades away in weeks 1–8, and NO_2 emission even slightly exceeds the corresponding 2019 level during the second eight weeks, although this gap is abated in the next eight weeks.

Because coal-fired power stations also produce NO_2, those results are subject to the qualification that the output of coal-fired power stations is accounted for when we associate NO_2 emission with traffic congestion. It is possible that the rise in coal-fired power caused the change in NO_2. To exclude this possibility, we make the following analysis.

First, we adopt a simple approach to make a comparison between daytime and nighttime NO_2. emission. Power engines usually do not stop during the night because of the high turn-on cost. As such, there should be no significant differences between daytime and nighttime emissions if emissions were mainly created by coal-fired power stations. However, traffic is usually not severe during the night, so there should be a significant difference between daytime and nighttime emission if emissions were mainly created by traffic. Columns (2)

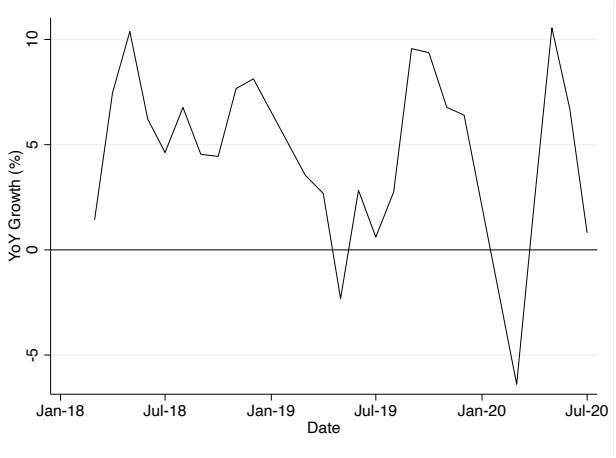

Figure 5: The Growth of Thermal Power

Note: Data are collected from the National Bureau of Statistics of China.

and (3) present the results of daytime and nighttime NO_2 emission, respectively. NO_2. emission declines in both daytime and nighttime, and the magnitudes are comparable during lockdown. However, daytime emission begins to increase ever since the start of reopening, but nighttime emission has stayed the same as in 2019. Those results show that the increase of NO_2. emission in the post-lockdown period cannot be fully explained by coal-fired power growth.

Second, we calculate the city-level coal-fired power capacity by exploiting a comprehensive coal plant dataset from the Global Coal Plant Tracker of Global Energy Monitor. As shown in Table A1, cities with a larger coal-fired power capacity tend to have higher NO_2 emission after the pandemic. However, when we control for the interaction term between power capacity and lunar calendar date, the coefficient of "Weeks >16" is still significantly positive for daytime NO_2.

Finally, statistical data shows that the growth rate of thermal power was not very high in 2020 (Figure 5). The only peak appeared in May, which is consistent with our regression results that NO_2 rebounds to a higher level during weeks 8–16. After that time, the growth of thermal power was limited and is unlikely to explain the rise of NO_2 after week 16.

Figure 6(a)-6(c) present the dynamic effects of the pandemic on NO_2, estimated from Equation 2 on the full sample. There is no pre-trend in any of the three averages. The post-lockdown effects present consistent but finer pictures than the DID results.

The lockdown effects estimated by the full sample are preserved when we study the weekday sample, but the effects for reopening are weaker. We find no significant coefficients for the 24-hour average emission, and the positive effect for daytime emission in the first eight weeks turns insignificant. In addition, we find that nighttime emission continues to decline

in the first eight weeks. Therefore, the results of the whole sample are largely contributed by the changes happening on weekends. This conclusion reinforces our hypothesis that the pandemic has changed people's travel patterns. During weekdays, people may opt for private transportation because of the pressure to rush to the workplace. During weekends, people do not have this pressure and the effects are more likely to reflect people's changes in travel patterns.

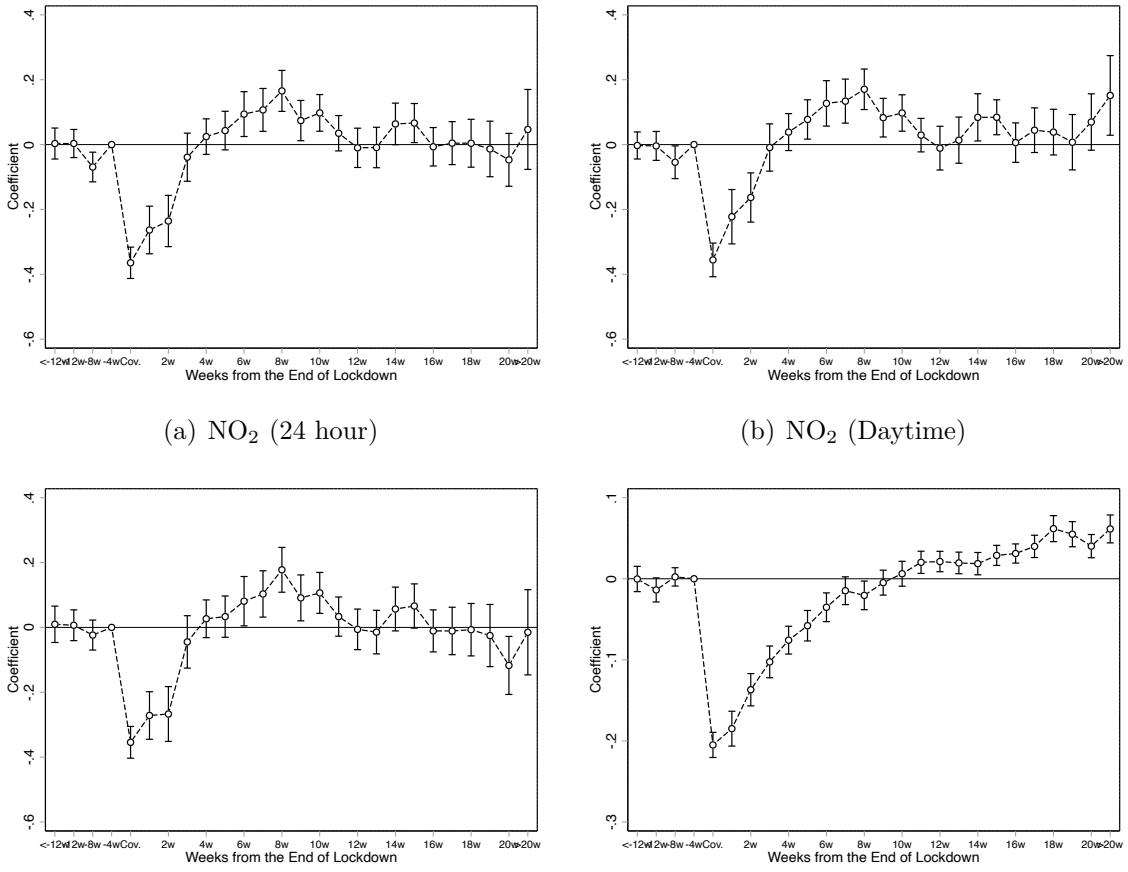

(a) NO_2 (24 hour)

(b) NO_2 (Daytime)

(c) NO_2 (Night)

(d) CDI

Figure 6: The Dynamic Impacts on Congestion and Pollution

Note: The coefficient estimates are obtained by estimating Equation (2). Vertical bands represent +(-)1.96 times the standard error of each point estimate. Standard errors are clustered at the city level. Daytime: 8:00–19:00h. Night: 0:00–8:00 and 19:00–24:00. The end of the lockdown period is collected from government websites and local news.

4.2 Traffic Congestion

Table 3 presents the results for traffic congestion. Again, we estimate Equation 1 using both the full sample and the weekday sample. The dependent variable is log-CDI. Column (1)

Table 3: The Results for Road Congestion

Outcome	Log Congestion Index	
	Full Sample	Weekdays Only
	(1)	(2)
Lockdown	-0.202***	-0.214***
	(0.000)	(0.000)
Weeks 1–8	-0.076***	-0.081***
	(0.000)	(0.000)
Weeks 9–16	0.020**	0.014*
	(0.002)	(0.048)
Weeks >16	0.053***	0.050***
	(0.000)	(0.000)
Observations	44,388	31,671
R^2	0.685	0.778

Note: *p*-values are reported in parentheses. Standard errors are clustered at the city level. Control variables include daily temperature, humidity, sea-level pressure, wind speed, wind direction, city-year fixed effects, and lunar calendar date fixed effects. Day: 8:00-19:00. Night: 0:00–8:00 and 19:00–24:00. Lockdown: lockdown period. * $p < 0.05$, ** $p < 0.01$, *** $p < 0.001$.

presents the results of the full sample. Compared to the pre-pandemic days, CDI decreases significantly by 20.2 percent during the lockdown period, and it continues to decrease by 7.6 percent in the first eight weeks after the termination of lockdown. However, road congestion begins to exceed the pre-pandemic level entering the second eight weeks after the end of lockdown. CDI increases by 2.0 percent in the second eight weeks after reopening and by 5.3 percent since the third eight weeks after reopening. The effects are significant at the 1 percent significance level. The results are robust when weekdays are studied (see Column (2)). According to the results for weekdays, on average, if people spent 1 hour on their daily commute in 2019, they would save about 10 minutes every day during the lockdown and 4 minutes within the first eight weeks after reopening, but they would spend an extra 3 minutes after that.

Figure 6(d) demonstrates the dynamic effects of COVID-19 on CDI by estimating Equation 2. The constant γ_0 is 0.47. The gap between 2019 and 2020 during the omitted period (–4 to –1 week) is –0.07 and is significant at the 0.001 level. The numbers shown in the figure are relative to this gap. The coefficients before the pandemic are close to zero, which suggests that there is no pre-treatment trend. Consistent with Table 3, the daily congestion index decreases significantly during the lockdown period, then gradually bounces back, recovers to the pre-pandemic level in the medium term, and finally exceeds the pre-pandemic level

in the long term. Overall, the results suggest that traffic congestion worsened in the long run, despite the temporary reduction during the lockdown period. The results are consistent with the pattern of changes in NO_2 emission when the capacity of coal-fired power plants is controlled for.

4.3 Robustness Checks

4.3.1 Expanding the Sample

In the aforementioned analysis, we have limited our analysis to cities without missing values in air pollution and CDI observations. Because the sample cities are mostly located in economically developed regions, there is a concern that our results are biased. For example, underdeveloped regions tend to have fewer power plants, factories, and vehicles, so the pandemic's impacts on travel behavior and air pollution are weaker. While we do not have nationwide CDI data, we can, however, expand the analysis on NO_2 to all cities with available air pollution data. As shown in Figure A1 and Table A2, the full sample includes 259 cities (78.5 percent of all the prefecture-level cities) and 141,932 city-day observations after excluding cities with too many missing values (as discussed in Section 3). Table A3 replicates the analysis on NO_2 by using the nationwide sample. Our baseline results are largely preserved.

4.3.2 An Alternative Definition of the Lockdown Period

In the previous analysis, the ending date of the lockdown, collected from government announcements and local news, was city-specific and varied from February to May 2020 (Figure 2). One potential problem with that definition is that the dates might be imprecise because of the limitation of the available information. For example, some cities regularly clear announcement archives on their government websites, and we must rely on other indirect policies, such as the end of their province's first-level responses, to infer the date. As a result, the assigned end dates could be different from the actual dates.

An alternative approach is to set a uniform ending date for all the cities. One of the choices is the date of the last reopening among the sample cities. But that choice may overstretch the lockdown in many cities because a few cities did not reopen until mid-May 2020 when new cases of infection of the initial wave of the pandemic had vanished long ago in the country. Instead, we chose March 18, 2020, as the uniform date for lockdown because on this day new confirmed cases were cleared. Figure A2 replicates the dynamic effects presented by Figure 6. As before, we observe a significant reduction in both congestion and

NO_2 in the lockdown period and increased congestion and daily NO_2 emission around the 16th week of reopening.

4.3.3 Impacts on Other Air Quality Measures

Do our results for NO_2 hold for other air quality measures? Unlike NO_2, which is mainly emitted by mobile vehicles, other pollutants, such as PM 2.5, SO_2, and CO, are generated by multiple sources. As a result, the impacts of the pandemic may be ambiguous (Almond et al., 2021; Ropkins and Tate, 2021). We study two indicators: Air Quality Index (AQI) and PM 2.5 density. Table A4. presents the results. Consistent with Almond et al. (2021) and He et al. (2020), we do find short-term improvements during the lockdown period, although their magnitudes and significance are much smaller than NO_2's. The short-term improvement of PM 2.5 disappears in the weekday subsample, though. In the longer term, the improvement is either unstable or nonexistent. Overall, our estimation finds short-term impacts but shaky long-term impacts for other pollutants. This finding can be contrasted with our early finding for NO_2. Resumed economic activities do not increase pollution after reopening, and more severe traffic congestion mainly causes rising NO_2 emission.

4.3.4 Remote Work

The pandemic has raised the popularity of remote working (Bartik et al., 2020; Brynjolfsson et al., n.d.; Dingel and Neiman, 2020). Recent studies show that remote working helps mitigate the impacts of the pandemic, especially on the labor market (Béland et al., 2020; Kalenkoski and Pabilonia, 2020). The literature shows that the spread of remote businesses improves air quality and alleviates traffic congestion (Pérez et al., 2004; Giovanis, 2018). Here we conduct a heterogeneous analysis and provide some preliminary evidence for the possible impacts of remote working on our baseline results. results.

Remote working is closely linked to the use of the internet. As a result, cities with better and wider internet penetration are expected to offer more remote working opportunities. We collect data for the internet penetration rate from the China Internet Network Information Center and measure the rate at the province level. We use the median rate of 2018 to classify cities into high and low groups. Table A5 presents the heterogeneous results for the two groups. The results are broadly consistent with our expectations. The reduction of NO_2 during lockdown is found to be more pronounced in the high-penetration group (Panel A) than in the low-penetration group (Panel B), and the increase after reopening is weaker in the former group than in the latter group. In cities with high internet penetration, lockdown encouraged more people to work from home, and this newly formed habit lasted after the

economy was reopened. In contrast, people in cities with low internet penetration stayed at home during lockdown more because of the government's restrictive policy and were more likely to go back to the workplace after reopening.

5 Travel Behavior

In this section, we explore a possible channel for worsening congestion after reopening: the shift in travel behavior. During the lockdown, two factors affected people's travel patterns. One is the government's restrictive policy, and the other is people's own fear of infection. Both factors lead to an overall reduction in travel—public transit and private vehicles alike. The second factor creates an additional structural effect that shifts people from public transit to private vehicles. Taking public transportation implies close-range contact with other people, thus drastically increasing a person's risk of infection. This concern would prompt people to opt for private vehicles. There are people who use their vehicles mainly for leisure and choose public transportation for their daily commute. The fear of infection, however, may lead those people to use their vehicles to commute between their home and workplace. It is noticeable that the fear is both real and psychological. The latter arises because the government's lockdown policy sends a strong message that the virus is pervasive and strongly contagious.

The first factor disappears when lockdown is lifted, but the second factor still exists as long as the virus is not eradicated. More important, the change from public transportation to private vehicles may persist because of the existence of actual and psychological costs of behavior adjustment. During the lockdown, the fear of infection is strong enough to overcome the adjustment costs associated with the change from public transportation to private vehicles. After reopening, the fear of infection declines, partly because of the relaxation of the government's restrictive policy and partly because of the drastic decline of new infection cases. Now the adjustment costs associated with reversing transit dominate and more private vehicles remain on the road than before.

Existing research does find that people tend to avoid public transportation and increase private vehicle usage during the outbreak of epidemics (Sadique et al., 2007; Abdullah et al., 2020; Kwok et al., 2020). However, there are no empirical studies showing whether the shift is temporary or persistent. In the next subsections, we use three sources of data to provide evidence for the persistence of the impact: administrative data, subway passenger flows in large cities, and heterogeneous results for NO_2 by the pre-pandemic density of public transit.

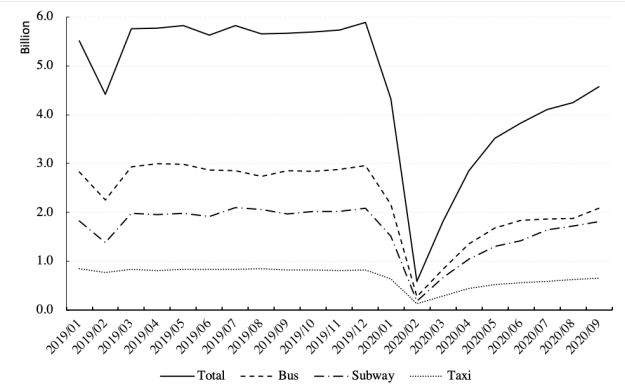

Figure 7: Monthly Public Transportation Volumes (2019–2020)
Source: Ministry of Transport of the People's Republic of China. Unit: 10,000 Persons

5.1 Administrative Data

Since 2019, the Ministry of Transport of the People's Republic of China has published monthly public transit volumes in 36 provincial cities and province capitals. Figure 7 shows the aggregate trend and allows us to observe the change of passenger flows before and after the pandemic. Passenger flows remained almost constant in 2019, except around the Spring Festival holiday in February. The outbreak of COVID-19 hit the public transportation system seriously. In February 2020, the number of passengers was reduced by more than 80 percent. It did not return to the pre-COVID level even in September, six months after the end of the nationwide pandemic.

China registered 2.4 percent year-on-year GDP growth in 2020. The drop in passenger volumes for public transportation after reopening did not fall in line with this growth. One explanation is that people have opted for private vehicles, which was reflected by rising auction prices of license plates in major cities. Many Chinese cities set up an auction system for license plates of private vehicles to control congestion. Auction prices reflect the local demand for private vehicles. Figure 8 shows the monthly auction prices between October 2019 and December 2021 in Shanghai and Guangzhou, two megacities that implement the auction policy.[1] In Shanghai, the auction price immediately increased after the outbreak of the pandemic and continued to rise until April 2021. Since then, the price dropped, but remained higher than the level of October 2019 until the end of 2021. In Guangzhou, the auction price experienced two spikes of growth since the outbreak of the pandemic, and like in Shanghai, the price remained higher than the level of October 2019 until the end of 2021. While the price increases during lockdown can be explained by people's fear of infection caused by public transportation, the long-lasting higher prices after reopening were more

[1] Unfortunately, only those two cities disclosed the auction prices.

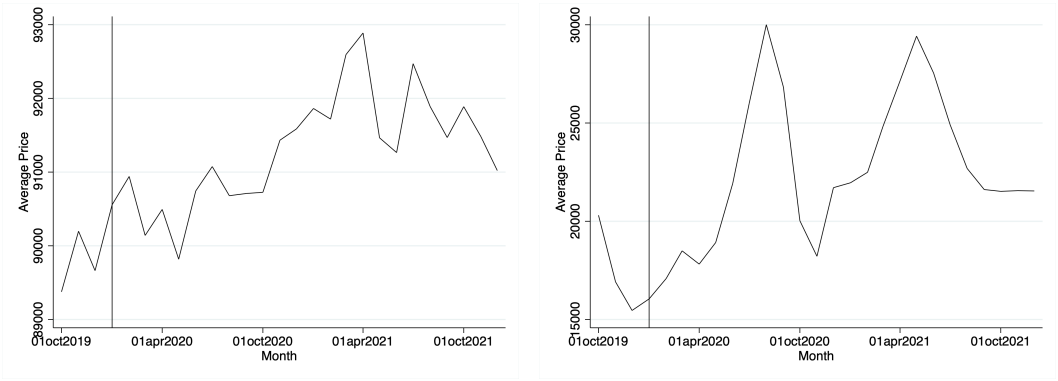

(a) Shanghai (b) Guangzhou

Figure 8: Auction Prices of License Plates in Two Megacities
Source: Shanghai Municipal Transportation Commission, Guangzhou Vehicle Regulation and Management Office. Unit: Yuan.

likely to be associated with people's changing habits to drive private vehicles for work and leisure.

5.2 Subway Passenger Flows

Next, we study the change in daily subway passenger flows. We obtain daily subway passenger flow data in eight major cities from Wind: Chongqing, Shanghai, Guangzhou, Nanning, Wuhan, Xi'an, Suzhou, and Zhengzhou. Except for Nanning, all the other cities are megacities with a population of more than 10 million people. For those megacities, we estimate Equation 1 for the congestion index and subway passenger volumes.[1] Table 4 displays the results, and Figure 9 visualizes the patterns. Columns (1) and (2) of Table 4 report the results. Similar to Figure 7, subway volumes dramatically dropped in 2020. Our results suggest that the volume drops by 87 percent during the lockdown period. It does not recover even after reopening. In the third eight-week period after the end of lockdown, subway volumes are still 22.7 percent lower than the pre-COVID level. The gaps are significant at the 0.1 percent level, even if there are only eight cities in the sample. On the contrary, the congestion index gradually rebounds and finally settles at a level 10.3 percent higher than the pre-COVID level. The results remain robust for weekdays (see Columns (3) and (4) in Table 4). The results are also robust under alternative definitions of lockdown (Figure A3). The divergent results for the congestion index and subway passenger volumes after reopening suggests that there is a long-term shift from public transit to private vehicles.

[1]We do not control for sea-level pressure here because of the missing value problem.

Table 4: The Substitution between Public Transportation and Private Vehicles

	Full Sample		Weekdays	
	Congestion	Subway	Congestion	Subway
	(1)	(2)	(3)	(4)
Lockdown	-0.226***	-2.118***	-0.226***	-1.965***
	(0.000)	(0.000)	(0.000)	(0.000)
Post1 (week 1-8)	-0.052	-0.940***	-0.024	-0.910***
	(0.055)	(0.000)	(0.335)	(0.000)
Post2 (week 9-16)	0.064**	-0.407***	0.066*	-0.455***
	(0.002)	(0.000)	(0.010)	(0.000)
Post3 (week >16)	0.103***	-0.227**	0.097**	-0.258***
	(0.000)	(0.003)	(0.002)	(0.000)
Observations	4,384	4,287	3,128	3,062
R^2	0.663	0.950	0.784	0.965

Note: p-values are reported in parentheses. Standard errors are clustered at the city level. Control variables include daily temperature, humidity, wind speed, wind direction, city-year fixed effects, and lunar calendar date fixed effects. Lockdown: lockdown period. * $p < 0.05$, ** $p < 0.01$, *** $p < 0.001$.

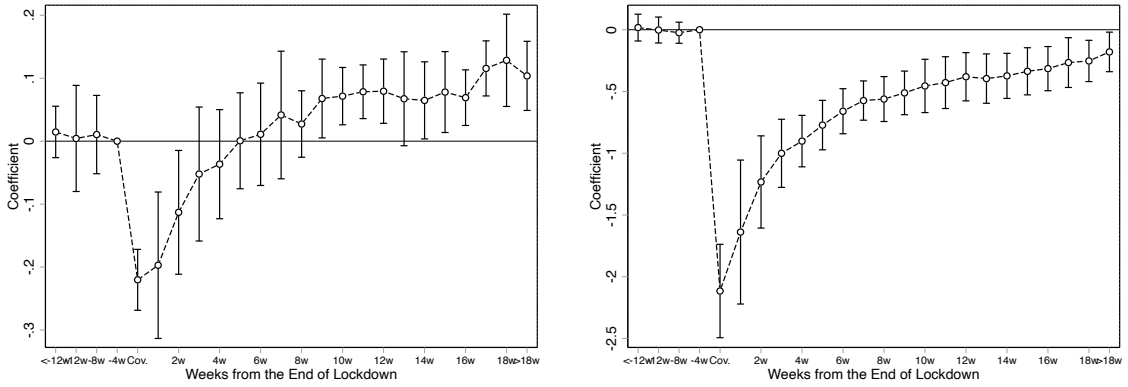

(a) CDI

(b) Subway Passenger Flow

Figure 9: The Shift of Travel Patterns

Note: The coefficient estimates are obtained by estimating Equation (2). Vertical bands represent +(-)1.96 times the standard error of each point estimate. Standard errors are clustered at the city level. The end of lockdown period is collected from government websites and local news.

5.3 Heterogeneous results for NO_2

Finally, we study the heterogeneous results for NO_2 in cities with different levels of pre-pandemic density of public transportation. It is reasonable to believe that the share of people shifting from public transit to private vehicles should be about the same across cities. Then in cities where people initially relied more on public transit, there would be more people shifting to private vehicles. To conduct our study, we expand our sample to all cities with available air pollution data, as in Section 4.3, to allow for more variations in the level of public transportation. We define the public transportation density as the public transport passenger volume divided by city population. The passenger volume and population are year-level data collected from city yearbooks. We divide the sample cities into two groups by the median of public transportation density in 2018. Table 5 presents the results of NO_2 for the two subgroups. The V-shaped dynamic is initially similar in the two subgroups but diverges after week 16. The estimate for NO_2 daytime concentration is positive and large in the high-density group (Panel A), but it is close to zero in the low-density group (Panel B). Because NO_2 concentration is directly linked to the number of vehicles, the heterogeneous effects found here are consistent with the idea that a higher density of public transit leads to a higher level of substitution between private vehicles and public transit.

5.4 Shift from Rush Hours to Slack Hours

The congestion index is constructed as a daily average. The distribution of traffic in rush hours and slack hours can affect the index. If that is the case, our results for the substitution between private and public transit must be qualified. In this subsection, we first study whether lockdown has changed that distribution and then discuss whether the change, if any, is sufficient to explain the increase of congestion after reopening.

We do not have hourly CDI data, so we study hourly NO_2 data. Rush hours are defined as 8–10 AM and 5–7 PM in a day and slack hours are defined as 11 AM–4 PM in a day. The daily average of NO_2 concentration during the rush or slack hours in a city is the dependent variable. Table 6 reports the results for the two daytime periods. NO_2 concentration does not increase significantly in rush hours after reopening but increases significantly in slack hours. This suggests that people shifted their day trips from rush hours to slack hours after reopening. One explanation is that people want to avoid large crowds in parking lots or other transit points. Another explanation is that companies and government agencies have allowed employees to have more flexible working hours, a habitual policy inherited from the lockdown.

Whether the shift from rush hours to slack hours can explain the increase in the daily

Table 5: Heterogeneous Effects for NO_2 by Public Transit Density

Outcome	Log NO_2					
	Full Sample			Weekdays Only		
	24h	Day	Night	24h	Day	Night
	(1)	(2)	(3)	(4)	(5)	(6)
Panel A. High Public Transit Density						
Lockdown	-0.306***	-0.297***	-0.310***	-0.282***	-0.257***	-0.280***
	(0.000)	(0.000)	(0.000)	(0.000)	(0.000)	(0.000)
Weeks 1–8	0.026	0.072***	0.001	0.002	0.065***	-0.020
	(0.162)	(0.000)	(0.963)	(0.925)	(0.001)	(0.348)
Weeks 9–16	0.082***	0.100***	0.069***	0.049**	0.084***	0.042*
	(0.000)	(0.000)	(0.000)	(0.004)	(0.000)	(0.017)
Weeks >16	0.047	0.116***	0.001	0.035	0.096**	0.006
	(0.074)	(0.000)	(0.962)	(0.232)	(0.001)	(0.863)
Observations	61,376	61,376	61,376	43,792	43,792	43,792
R^2	0.678	0.664	0.641	0.687	0.671	0.650
Panel B. Low Public Transit Density						
Lockdown	-0.349***	-0.319***	-0.370***	-0.304***	-0.261***	-0.321***
	(0.000)	(0.000)	(0.000)	(0.000)	(0.000)	(0.000)
Weeks 1–8	0.013	0.047*	-0.015	-0.010	0.040*	-0.037
	(0.458)	(0.020)	(0.457)	(0.569)	(0.045)	(0.071)
Weeks 9–16	0.044*	0.055*	0.024	0.016	0.052*	-0.007
	(0.029)	(0.016)	(0.229)	(0.425)	(0.024)	(0.733)
Weeks >16	-0.027	0.008	-0.063*	-0.017	0.019	-0.050
	(0.314)	(0.799)	(0.020)	(0.560)	(0.530)	(0.094)
Observations	65,212	65,212	65,212	46,529	46,529	46,529
R^2	0.676	0.657	0.641	0.683	0.664	0.647

Note: *p*-values are reported in parentheses. Standard errors are clustered at the city level. Control variables include daily temperature, humidity, sea-level pressure, wind speed, wind direction, city-year fixed effects, and lunar calendar date fixed effects. Public Transit Density: public transit passenger volume divided by city population in 2018. The cutoff is the median public transit density. Day: 8:00-19:00. Night: 0:00–8:00 and 19:00–24:00. Lockdown: lockdown period. * $p < 0.05$, ** $p < 0.01$, *** $p < 0.001$.

Table 6: The Impacts on NO_2, Rush Hours versus Slack Hours

Outcome	Log NO_2					
	Full Sample			Weekdays Only		
	Daytime (1)	Rush Hours (2)	Slack Hours (3)	Daytime (4)	Rush Hours (5)	Slack Hours (6)
Lockdown	-0.342***	-0.356***	-0.327***	-0.283***	-0.307***	-0.261***
	(0.000)	(0.000)	(0.000)	(0.000)	(0.000)	(0.000)
Weeks 1–8	0.028	0.000	0.048*	0.014	-0.028	0.043
	(0.194)	(0.992)	(0.036)	(0.541)	(0.178)	(0.086)
Weeks 9–16	0.060**	0.036*	0.076***	0.059**	0.023	0.084***
	(0.002)	(0.044)	(0.000)	(0.003)	(0.212)	(0.000)
Weeks >16	0.065*	0.015	0.091*	0.045	-0.008	0.082*
	(0.046)	(0.618)	(0.010)	(0.193)	(0.806)	(0.028)
Observations	44,388	44,388	44,388	31,671	31,671	31,671
R^2	0.669	0.671	0.641	0.676	0.681	0.647

Note: *p*-values are reported in parentheses. Standard errors are clustered at the city level. Control variables include daily temperature, humidity, sea-level pressure, wind speed, wind direction, city-year fixed effects, and lunar calendar date fixed effects. Day: 8:00-19:00. Rush Hours: 8:00-10:00 and 17:00-19:00. Slack Hours: 10:00-17:00. Lockdown: lockdown period. * $p < 0.05$, ** $p < 0.01$, *** $p < 0.001$.

average congestion depends on whether the shift has increased the total amount of travel time in a day. If the volume of the shift is in a range such that the travel time (congestion) during rush hours declines but travel time (congestion) during slack hours does not increase, then the amount of travel time (congestion) in a day should be reduced. For the shift to explain the rise of average congestion in a day, travel time (congestion) during slack hours must have increased sufficiently. As discussed in Table 3, the daily congestion index rises by 5 percent on average. Suppose the rise in daily congestion is merely driven by the shift of travel time. Since slack hours only last for 7 hours, less than a third of the day, congestion during slack hours should rise by at least 15 percent. This prediction, however, conflicts with the real case. Let's look at Xi'an, the megacity that suffered the most severe congestion in the third quarter of 2020, as an example.[1]. Although congestion during slack hours is severely worsened in Xi'an, the rise in the congestion index is still less than 15 percent compared to the third quarter of 2019—approximately from 1.5 to 1.7. Besides, the rush-hour congestion index also keeps going up, contrary to the prediction that the congestion during rush hours would be relieved. Therefore, the shift of travel time alone is not sufficient to explain the patterns in congestion.

[1]See Gaode Map, "Traffic Analysis Report of Major Cities in China, 2020Q3" (in Chinese), https://report.amap.com/download_city.do

6 Conclusion

The COVID-19 pandemic is reshaping human behavior across the world. In this study, we first investigate its impacts on air pollution and road congestion in Chinese cities. We find that the pandemic has generated opposite effects during and after the lockdown period. In the short run, the public reduced its mobility in response to the pandemic and government lockdown policies, which led to a temporary but dramatic drop in travel and NO_2 emission. However, road congestion and NO_2 concentration worsened after society reopened. We find evidence that changed human travel behavior created this contrast. In a response to the risk of being infected, people switched their modes of travel from public transit to private vehicles during the lockdown, and this switch has persisted after society reopened.

Our study suggests that the COVID-19 pandemic is far more than a temporary shock. Its direct impacts may fade out as the pandemic ends, but the changes in human behavior can persist and continue to affect everyday life. Our study has found that the pandemic has changed people's travel patterns, most likely by changing people's perception of the chance of being infected, and this change persists after the nationwide pandemic is being controlled. The switch to private vehicles poses a new challenge to public transportation and emission reduction. It is a new issue for researchers and policymakers to figure out how to recover people's confidence in and their demand for public transit after the pandemic.

References

Abdullah, Muhammad, Charitha Dias, Deepti Muley, and Md Shahin, "Exploring the impacts of COVID-19 on travel behavior and mode preferences," *Transportation Research Interdisciplinary Perspectives*, 2020, *8*, 100255–100255.

Almond, Douglas, Xinming Du, Valerie J Karplus, and Shuang Zhang, "Ambiguous Air Pollution Effects of China's COVID-19 Lock-Down," in "AEA Papers and Proceedings," Vol. 111 2021, pp. 376–80.

Anderson, Michael L, "Subways, strikes, and slowdowns: The impacts of public transit on traffic congestion," *American Economic Review*, 2014, *104* (9), 2763–96.

Bartik, Alexander W, Zoe B Cullen, Edward L Glaeser, Michael Luca, and Christopher T Stanton, "What jobs are being done at home during the COVID-19 crisis? Evidence from firm-level surveys," Technical Report, National Bureau of Economic Research 2020.

Bel, Germà and Maximilian Holst, "Evaluation of the impact of bus rapid transit on air pollution in Mexico City," *Transport Policy*, 2018, *63*, 209–220.

Brodeur, Abel, Nikolai Cook, and Taylor Wright, "On the effects of COVID-19 safer-at-home policies on social distancing, car crashes and pollution," *Journal of environmental economics and management*, 2021, *106*, 102427.

Brynjolfsson, E., J. J. Horton, A. Ozimek, D. Rock, G. Sharma, and Hy Tu Ye, "Covid-19 and Remote Work: An Early Look at Us Data," *Social Science Electronic Publishing.*

Bucsky, Péter, "Modal share changes due to COVID-19: The case of Budapest," *Transportation Research Interdisciplinary Perspectives*, 2020, *8*, 100141–100141.

Béland, Louis-Philippe, Abel Brodeur, and Taylor Wright, "The Short-Term Economic Consequences of COVID-19: Exposure to Disease, Remote Work and Government Response," GLO Discussion Paper Series 524, Global Labor Organization (GLO) 2020.

Chan, Chak K and Xiaohong Yao, "Air pollution in mega cities in China," *Atmospheric environment*, 2008, *42* (1), 1–42.

Chay, Kenneth, Carlos Dobkin, and Michael Greenstone, "The Clean Air Act of 1970 and adult mortality," *Journal of risk and uncertainty*, 2003, *27* (3), 279–300.

Chay, Kenneth Y and Michael Greenstone, "The impact of air pollution on infant mortality: evidence from geographic variation in pollution shocks induced by a recession," *The quarterly journal of economics*, 2003, *118* (3), 1121–1167.

Chen, Simiao, Zongjiu Zhang, Juntao Yang, Jian Wang, Xiaohui Zhai, Till Bärnighausen, and Chen Wang, "Fangcang shelter hospitals: a novel concept for responding to public health emergencies," *The Lancet*, 2020, *395* (10232), 1305–1314.

Chen, Yihsu and Alexander Whalley, "Green infrastructure: The effects of urban rail transit on air quality," *American Economic Journal: Economic Policy*, 2012, *4* (1), 58–97.

Chen, Yuyu, Avraham Ebenstein, Michael Greenstone, and Hongbin Li, "Evidence on the impact of sustained exposure to air pollution on life expectancy from China's Huai River policy," *Proceedings of the National Academy of Sciences*, 2013, *110* (32), 12936–12941.

Chinazzi, Matteo, Jessica T Davis, Marco Ajelli, Corrado Gioannini, Maria Litvinova, Stefano Merler, Ana Pastore y Piontti, Kunpeng Mu, Luca Rossi,

Kaiyuan Sun et al., "The effect of travel restrictions on the spread of the 2019 novel coronavirus (COVID-19) outbreak," *Science*, 2020, *368* (6489), 395–400.

Currie, Janet and Matthew Neidell, "Air pollution and infant health: what can we learn from California's recent experience?," *The Quarterly Journal of Economics*, 2005, *120* (3), 1003–1030.

_ and Reed Walker, "Traffic congestion and infant health: Evidence from E-ZPass," *American Economic Journal: Applied Economics*, 2011, *3* (1), 65–90.

_ , Matthew Neidell, and Johannes F Schmieder, "Air pollution and infant health: Lessons from New Jersey," *Journal of health economics*, 2009, *28* (3), 688–703.

Dang, Hai-Anh and Trong-Anh Trinh, "The beneficial impacts of covid-19 lockdowns on air pollution: Evidence from vietnam," 2020.

Deryugina, Tatyana, Garth Heutel, Nolan H Miller, David Molitor, and Julian Reif, "The mortality and medical costs of air pollution: Evidence from changes in wind direction," *American Economic Review*, 2019, *109* (12), 4178–4219.

Deschenes, Olivier, Michael Greenstone, and Joseph S Shapiro, "Defensive investments and the demand for air quality: Evidence from the NOx budget program," *American Economic Review*, 2017, *107* (10), 2958–89.

Dingel, Jonathan I and Brent Neiman, "How many jobs can be done at home?," *Journal of Public Economics*, 2020, *189*, 104235.

Eidelman, Scott and Christian S Crandall, "A psychological advantage for the status quo," *Social and psychological bases of ideology and system justification*, 2009, pp. 85–106.

Fan, Cheng, Ying Li, Jie Guang, Zhengqiang Li, Abdelrazek Elnashar, Mona Allam, and Gerrit de Leeuw, "The impact of the control measures during the COVID-19 outbreak on air pollution in China," *Remote Sensing*, 2020, *12* (10), 1613.

Gendron-Carrier, Nicolas, Marco Gonzalez-Navarro, Stefano Polloni, and Matthew A Turner, "Subways and urban air pollution," Technical Report, National Bureau of Economic Research 2018.

Giovanis, Eleftherios, "The relationship between teleworking, traffic and air pollution," *Atmospheric pollution research*, 2018, *9* (1), 1–14.

Gu, Yizhen, Chang Jiang, Junfu Zhang, and Ben Zou, "Subways and road congestion," *American Economic Journal: Applied Economics*, 2021, *13* (2), 83–115.

He, Guojun, Yuhang Pan, and Takanao Tanaka, "The short-term impacts of COVID-19 lockdown on urban air pollution in China," *Nature Sustainability*, 2020, *3* (12), 1005–1011.

Ju, Min Jae, Jaehyun Oh, and Yoon-Hyeong Choi, "Changes in air pollution levels after COVID-19 outbreak in Korea," *Science of the Total Environment*, 2021, *750*, 141521.

Kalenkoski, Charlene Marie and Sabrina Wulff Pabilonia, "Initial Impact of the COVID-19 Pandemic on the Employment and Hours of Self- Employed Coupled and Single Workers by Gender and Parental Status," *IZA DP No. 13443*, 2020.

Kerr, Gaige H., Daniel L. Goldberg, and Susan C. Anenberg, "COVID-19 pandemic reveals persistent disparities in nitrogen dioxide pollution," *Proceedings of the National Academy of Sciences - PNAS*, 2021, *118* (30), 1.

Kim, Chansung, Seung Hoon Cheon, Keechoo Choi, Chang-Hyeon Joh, and Hyuk-Jin Lee, "Exposure to fear: Changes in travel behavior during MERS outbreak in Seoul," *KSCE Journal of Civil Engineering*, 2017, *21* (7), 2888–2895.

Kwok, Kin O., Kin K. Li, Henry H. H. Chan, Yuan Y. Yi, Arthur Tang, Wan I. Wei, and Samuel Y. S. Wong, "Community Responses during Early Phase of COVID-19 Epidemic, Hong Kong," *Emerging infectious diseases*, 2020, *26* (7), 1575–1579.

Li, Jian, Pengfei Xu, and Weifeng Li, "Urban road congestion patterns under the COVID-19 pandemic: A case study in Shanghai," *International Journal of Transportation Science and Technology*, 2021, *10* (2), 212–222.

Li, Shanjun, Yanyan Liu, Avralt-Od Purevjav, and Lin Yang, "Does subway expansion improve air quality?," *Journal of Environmental Economics and Management*, 2019, *96*, 213–235.

Liu, Luyu, Harvey J Miller, and Jonathan Scheff, "The impacts of COVID-19 pandemic on public transit demand in the United States," *Plos one*, 2020, *15* (11), e0242476.

Ming, Wen, Zhengqing Zhou, Hongshan Ai, Huimin Bi, and Yuan Zhong, "COVID-19 and air quality: Evidence from China," *Emerging Markets Finance and Trade*, 2020, *56* (10), 2422–2442.

Moretti, Enrico and Matthew Neidell, "Pollution, health, and avoidance behavior evidence from the ports of Los Angeles," *Journal of human Resources*, 2011, *46* (1), 154–175.

Otmani, Anas, Abdelfettah Benchrif, Mounia Tahri, Moussa Bounakhla, Mohammed El Bouch, M'hamed Krombi et al., "Impact of Covid-19 lockdown on PM10, SO2 and NO2 concentrations in Salé City (Morocco)," *Science of the total environment*, 2020, *735*, 139541.

Pan, An, Li Liu, Chaolong Wang, Huan Guo, Xingjie Hao, Qi Wang, Jiao Huang, Na He, Hongjie Yu, Xihong Lin et al., "Association of public health interventions with the epidemiology of the COVID-19 outbreak in Wuhan, China," *Jama*, 2020, *323* (19), 1915–1923.

Pérez, Manuela Pérez, Angel Martínez Sánchez, María Pilar de Luis Carnicer, and María José Vela Jiménez, "The environmental impacts of teleworking: A model of urban analysis and a case study," *Management of Environmental Quality: An International Journal*, 2004.

Ropkins, Karl and James E Tate, "Early observations on the impact of the COVID-19 lockdown on air quality trends across the UK," *Science of the Total Environment*, 2021, *754*, 142374.

Sadique, M. Z., W. J. Edmunds, Richard D. Smith, William J. Meerding, Onno De Zwart, Johannes Brug, and Philippe Beutels, "Precautionary behavior in response to perceived threat of pandemic influenza," *Emerging infectious diseases*, 2007, *13* (9), 1307–1313.

Samuelson, William and Richard Zeckhauser, "Status quo bias in decision making," *Journal of risk and uncertainty*, 1988, *1* (1), 7–59.

Shapiro, Robert J, Kevin A Hassett, and Frank S Arnold, "Conserving energy and preserving the environment: The role of public transportation," 2016.

Singh, Ramesh P and Akshansha Chauhan, "Impact of lockdown on air quality in India during COVID-19 pandemic," *Air Quality, Atmosphere & Health*, 2020, *13* (8), 921–928.

Sun, Chuanwang, Wenyue Zhang, Xingming Fang, Xiang Gao, and Meilian Xu, "Urban public transport and air quality: Empirical study of China cities," *Energy Policy*, 2019, *135*, 110998.

_ , Yuan Luo, and Jianglong Li, "Urban traffic infrastructure investment and air pol-

lution: Evidence from the 83 cities in China," *Journal of Cleaner Production*, 2018, *172*, 488–496.

Tian, Huaiyu, Yonghong Liu, Yidan Li, Chieh-Hsi Wu, Bin Chen, Moritz UG Kraemer, Bingying Li, Jun Cai, Bo Xu, Qiqi Yang et al., "An investigation of transmission control measures during the first 50 days of the COVID-19 epidemic in China," *Science*, 2020, *368* (6491), 638–642.

Topalovic, P, J Carter, M Topalovic, and G Krantzberg, "Light rail transit in Hamilton: Health, environmental and economic impact analysis," *Social Indicators Research*, 2012, *108* (2), 329–350.

Venter, Zander S., Kristin Aunan, Sourangsu Chowdhury, and Jos Lelieveld, "COVID-19 lockdowns cause global air pollution declines," *Proceedings of the National Academy of Sciences - PNAS*, 2020, *117* (32), 18984–18990.

Yan, Chaode, Xiaobing Wei, Xiao Liu, Zhiguo Liu, Jinxi Guo, Ziwei Li, Yan Lu, and Xiaohui He, "A new method for real-time evaluation of urban traffic congestion: a case study in Xi'an, China," *Geocarto International*, 2020, *35* (10), 1033–1048.

Yang, F, J Tan, Q Zhao, Z Du, K He, Y Ma, F Duan, and GJAC Chen, "Characteristics of PM 2.5 speciation in representative megacities and across China," *Atmospheric Chemistry and Physics*, 2011, *11* (11), 5207–5219.

Zhang, Kai and Stuart Batterman, "Air pollution and health risks due to vehicle traffic," *Science of the total Environment*, 2013, *450*, 307–316.

Appendix A. Figures

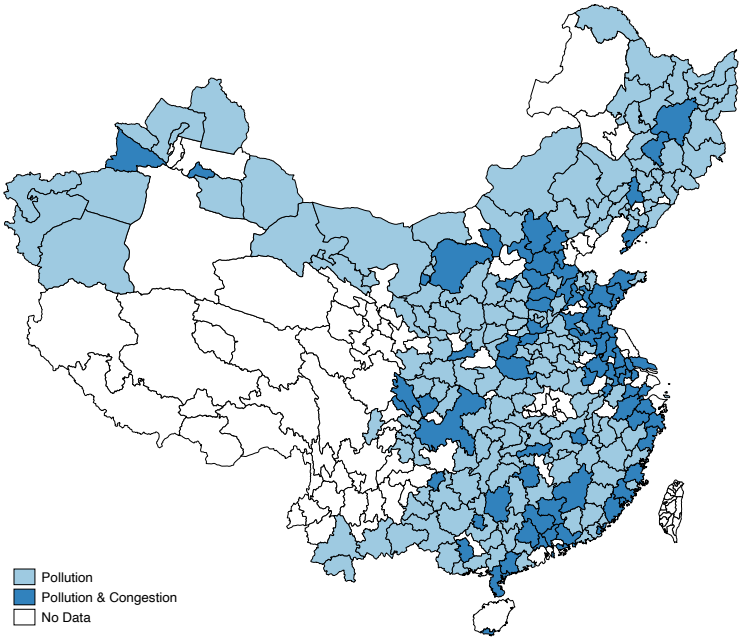

Figure A1: Cities in the Extended Sample

(a) CDI

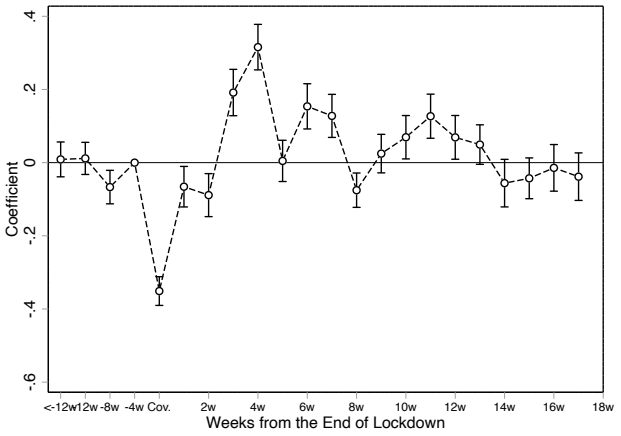

(b) NO_2 (24h)

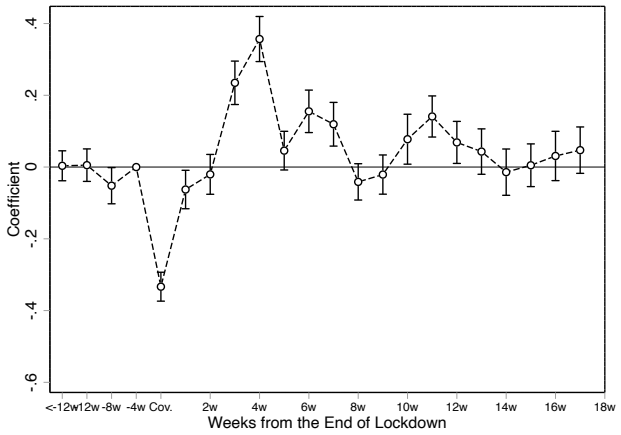

(c) NO_2 (Daytime)

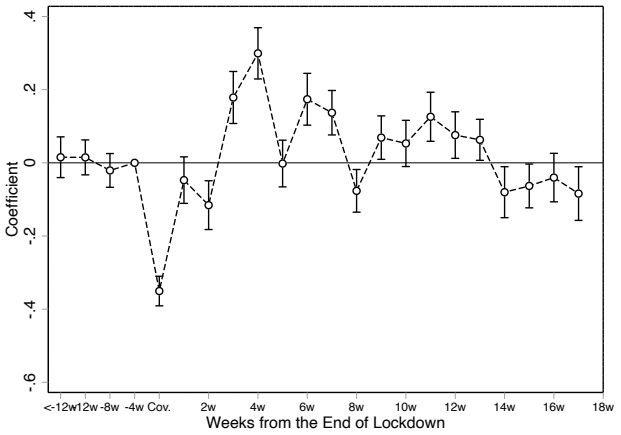

(d) NO_2 (Night)

Figure A2: The Dynamic Effects (Alternative Definition of Lockdown)

Note: The coefficient estimates are obtained by estimating Equation (2) . Vertical bands represent +(-)1.96 times the standard error of each point estimate. Standard errors are clustered at the city level. Daytime:8:00–19:00. Night: 0:00–8:00 and 19:00–24:00. The end of lockdown period is unified to March 19.

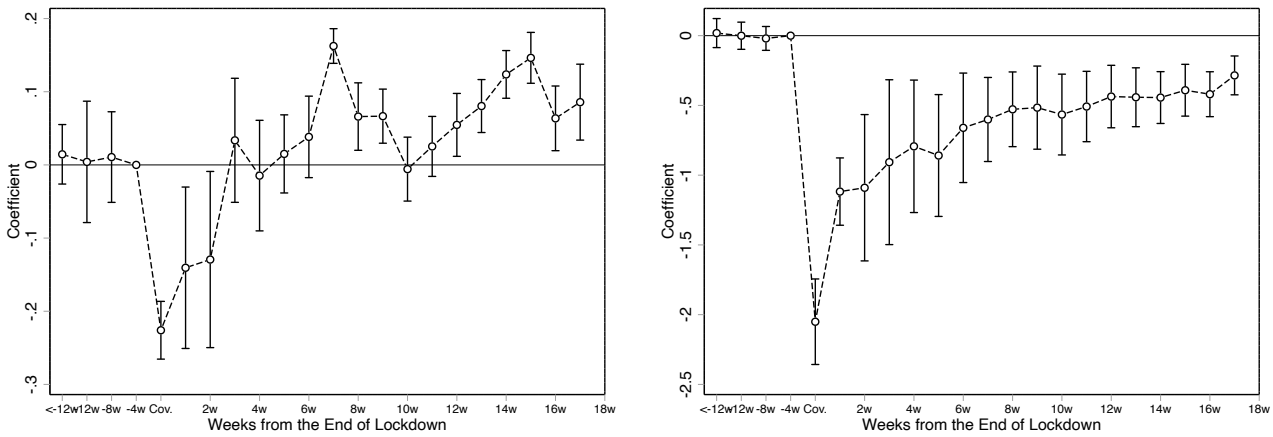

(a) CDI

(b) Subway Passenger Flow

Figure A3: The Shift of Travel Patterns (Alternative Definition of Lockdown)

Note: The coefficient estimates are obtained by estimating Equation (2). Vertical bands represent +(-)1.96 times the standard error of each point estimate. Standard errors are clustered at the city level. The end of lockdown period is unified to March 19.

Appendix B. Tables

Table A1: Controlling Coal-Fired Power Capacity

Outcome	Log NO_2					
	Full Sample			Weekdays Only		
	24h	Day	Night	24h	Day	Night
	(1)	(2)	(3)	(4)	(5)	(6)
Panel A. Subsample: High Coal-Fired Power Capacity						
Lockdown	-0.350***	-0.324***	-0.360***	-0.302***	-0.266***	-0.306***
	(0.000)	(0.000)	(0.000)	(0.000)	(0.000)	(0.000)
Weeks 1–8	-0.011	0.027	-0.041	-0.061	-0.008	-0.091*
	(0.758)	(0.447)	(0.277)	(0.092)	(0.821)	(0.022)
Weeks 9–16	0.071**	0.080**	0.051	0.033	0.072*	0.008
	(0.009)	(0.003)	(0.082)	(0.252)	(0.012)	(0.805)
Weeks >16	0.047	0.103*	-0.002	0.027	0.073	-0.009
	(0.307)	(0.033)	(0.976)	(0.605)	(0.184)	(0.878)
Observations	20,276	20,276	20,276	14,467	14,467	14,467
R^2	0.626	0.628	0.588	0.636	0.635	0.599
Panel B. Subsample: Low Coal-Fired Power Capacity						
Lockdown	-0.373***	-0.382***	-0.372***	-0.333***	-0.325***	-0.328***
	(0.000)	(0.000)	(0.000)	(0.000)	(0.000)	(0.000)
Weeks 1–8	-0.013	0.005	-0.026	-0.031	0.012	-0.041
	(0.659)	(0.872)	(0.436)	(0.338)	(0.707)	(0.262)
Weeks 9–16	0.032	0.038	0.024	-0.001	0.040	-0.014
	(0.216)	(0.185)	(0.399)	(0.970)	(0.167)	(0.637)
Weeks >16	-0.014	0.034	-0.054	-0.031	0.018	-0.063
	(0.727)	(0.469)	(0.206)	(0.492)	(0.691)	(0.221)
Observations	21,372	21,372	21,372	15,249	15,249	15,249
R^2	0.692	0.678	0.652	0.700	0.687	0.660
Panel C. Full Sample: Controlling for Volumn-Date Variables						
Lockdown	-0.348***	-0.341***	-0.353***	-0.304***	-0.282***	-0.303***
	(0.000)	(0.000)	(0.000)	(0.000)	(0.000)	(0.000)
Weeks 1–8	0.000	0.031	-0.021	-0.034	0.016	-0.053*
	(0.989)	(0.170)	(0.378)	(0.143)	(0.477)	(0.036)
Weeks 9–16	0.054**	0.062**	0.041*	0.021	0.061**	0.003
	(0.003)	(0.001)	(0.038)	(0.268)	(0.002)	(0.872)
Weeks >16	0.012	0.067*	-0.032	-0.006	0.047	-0.041
	(0.702)	(0.041)	(0.324)	(0.863)	(0.179)	(0.277)
Observations	44,388	44,388	44,388	31,671	31,671	31,671
R^2	0.682	0.672	0.644	0.690	0.679	0.652

Note: *p*-values are reported in parentheses. Standard errors are clustered at the city level. Control variables include daily temperature, humidity, sea-level pressure, wind speed, wind direction, city-year fixed effects, and lunar calendar date fixed effects. Day: 8:00-19:00. Night: 0:00–8:00 and 19:00–24:00. Lockdown: lockdown period. * $p < 0.05$, ** $p < 0.01$, *** $p < 0.001$.

Table A2: Summary Statistics (Nationwide)

Variable	Obs	Mean	Std. dev.	Min	Max
NO_2, 24h Average ($\mu g/m^3$)	141,932	27.42	15.63	1.00	128.00
NO_2, Daytime ($\mu g/m^3$)	141,932	23.34	14.46	1.00	138.45
NO_2, Night ($\mu g/m^3$)	141,932	30.69	17.95	1.00	159.62
Air Temperature	141,932	12.97	11.18	-37.12	40.06
Dew Point Temperature	141,932	5.63	12.66	-41.12	28.85
Sea-level Pressure	141,932	1,017.38	10.19	975.68	1,057.01
Wind Direction	141,932	173.81	66.57	0.00	360.00
Wind Speed	141,932	2.43	1.23	0.00	18.00
Precipitation	141,932	2.41	8.61	0.00	364.80
Public Transit Density	126,588	43.89	61.46	0.36	478.02

Table A3: The Impacts on NO_2 (Extended Sample)

Outcome	Log NO_2					
	Full Sample			Weekdays Only		
	24h	Day	Night	24h	Day	Night
	(1)	(2)	(3)	(4)	(5)	(6)
Lockdown	-0.335***	-0.314***	-0.349***	-0.304***	-0.269***	-0.314***
	(0.000)	(0.000)	(0.000)	(0.000)	(0.000)	(0.000)
Weeks 1–8	-0.001	0.040**	-0.029	-0.024	0.034*	-0.049**
	(0.956)	(0.005)	(0.051)	(0.092)	(0.020)	(0.001)
Weeks 9–16	0.045***	0.058***	0.030*	0.016	0.048**	0.002
	(0.001)	(0.000)	(0.029)	(0.252)	(0.002)	(0.894)
Weeks >16	-0.000	0.046*	-0.040*	0.002	0.042	-0.027
	(0.987)	(0.026)	(0.042)	(0.929)	(0.056)	(0.223)
Observations	141,932	141,932	141,932	101,269	101,269	101,269
R^2	0.685	0.663	0.651	0.691	0.669	0.658

Note: *p*-values are reported in parentheses. Standard errors are clustered at the city level. Control variables include daily temperature, humidity, sea-level pressure, wind speed, wind direction, city-year fixed effects, and lunar calendar date fixed effects. Day: 8:00-19:00. Night: 0:00–8:00 and 19:00–24:00. Lockdown: lockdown period. * $p < 0.05$, ** $p < 0.01$, *** $p < 0.001$.

Table A4: The Impacts on Other Air Quality Measurements

Outcome	Log PM 2.5						Log AQI	
	Full Sample			Weekdays Only			Full	Weekdays
	24h	Day	Night	24h	Day	Night	24h	
	(1)	(2)	(3)	(4)	(5)	(6)	(7)	(8)
Lockdown	-0.066*	-0.066*	-0.062*	-0.008	0.001	0.005	-0.101***	-0.095***
	(0.017)	(0.014)	(0.023)	(0.787)	(0.979)	(0.885)	(0.000)	(0.001)
Weeks 1–8	0.048	0.063*	0.040	0.013	0.050	0.004	-0.054*	-0.090**
	(0.109)	(0.047)	(0.165)	(0.717)	(0.176)	(0.907)	(0.024)	(0.001)
Weeks 9–16	0.046	0.057	0.032	0.005	0.032	-0.000	0.012	-0.026
	(0.111)	(0.069)	(0.242)	(0.871)	(0.351)	(0.996)	(0.605)	(0.326)
Weeks >16	-0.077*	-0.073	-0.103**	-0.118**	-0.097*	-0.148***	-0.029	-0.051
	(0.047)	(0.060)	(0.010)	(0.006)	(0.025)	(0.001)	(0.377)	(0.144)
Observations	44,388	44,388	44,388	31,671	31,671	31,671	44,388	31,671
R^2	0.553	0.501	0.550	0.565	0.509	0.563	0.519	0.531

Note: *p*-values are reported in parentheses. Standard errors are clustered at the city level. Control variables include daily temperature, humidity, sea-level pressure, wind speed, wind direction, city-year fixed effects, and lunar calendar date fixed effects. Day: 8:00-19:00. Night: 0:00–8:00 and 19:00–24:00. Lockdown: lockdown period. * $p < 0.05$, ** $p < 0.01$, *** $p < 0.001$.

Table A5: Heterogeneous Effects for NO_2 by Provincial Internet Penetration

Outcome	Log NO_2					
	Full Sample			Weekdays Only		
	24h	Day	Night	24h	Day	Night
	(1)	(2)	(3)	(4)	(5)	(6)
Panel A. High Internet Penetration Rate						
Lockdown	-0.367***	-0.363***	-0.374***	-0.326***	-0.302***	-0.332***
	(0.000)	(0.000)	(0.000)	(0.000)	(0.000)	(0.000)
Weeks 1–8	0.011	0.032	-0.010	-0.007	0.038*	-0.027
	(0.522)	(0.075)	(0.564)	(0.690)	(0.037)	(0.152)
Weeks 9–16	0.061***	0.060***	0.052**	0.023	0.046**	0.011
	(0.000)	(0.001)	(0.002)	(0.157)	(0.010)	(0.508)
Weeks >16	-0.010	0.018	-0.043	-0.014	0.017	-0.042
	(0.710)	(0.531)	(0.110)	(0.624)	(0.569)	(0.169)
Observations	75,624	75,624	75,624	53,958	53,958	53,958
R^2	0.687	0.664	0.654	0.695	0.673	0.663
Panel B. Low Internet Penetration Rate						
Lockdown	-0.287***	-0.249***	-0.308***	-0.263***	-0.217***	-0.275***
	(0.000)	(0.000)	(0.000)	(0.000)	(0.000)	(0.000)
Weeks 1–8	0.006	0.064**	-0.023	-0.019	0.047*	-0.042
	(0.785)	(0.007)	(0.322)	(0.402)	(0.048)	(0.075)
Weeks 9–16	0.044	0.062*	0.031	0.024	0.056*	0.017
	(0.052)	(0.015)	(0.169)	(0.327)	(0.041)	(0.465)
Weeks >16	0.024	0.086**	-0.016	0.034	0.079*	0.011
	(0.386)	(0.005)	(0.563)	(0.249)	(0.017)	(0.707)
Observations	66,308	66,308	66,308	47,311	47,311	47,311
R^2	0.703	0.680	0.671	0.710	0.687	0.679

Note: *p*-values are reported in parentheses. Standard errors are clustered at the city level. Control variables include daily temperature, humidity, sea-level pressure, wind speed, wind direction, city-year fixed effects, and lunar calendar date fixed effects. Province Internet Penetration Rates are collected from the China Internet Network Information Center. The cutoff is the median of Internet Penetration Rate. Day: 8:00-19:00. Night: 0:00–8:00 and 19:00–24:00. Lockdown: lockdown period. * $p < 0.05$, ** $p < 0.01$, *** $p < 0.001$.